

Transient Absorption Imaging of P3HT:PCBM Photovoltaic Blend: Evidence For Interfacial Charge Transfer State

Giulia Grancini,[†] Dario Polli,^{†,‡} Daniele Fazzi,[†] Juan Cabanillas-Gonzalez,[§] Giulio Cerullo,[†] and Guglielmo Lanzani^{*,†,‡}

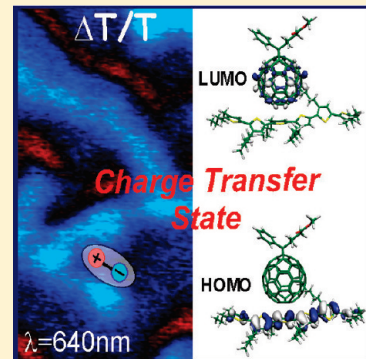
[†]IFN-CNR, Dipartimento di Fisica, Politecnico di Milano, Piazza L. da Vinci, 32, 20133 Milano, Italy

[‡]Center for NanoScience and Technology CNST-IIT@POLIMI, via Pascoli 70/3, 20133 Milano, Italy

[§]Madrid Institute of Advanced Studies, IMDEA Nanociencia, Facultad de Ciencias, Avenida Tomas y Valiente 7, 28049 Madrid, Spain

 Supporting Information

ABSTRACT: Solution-processed bulk heterojunction (BHJ) based on electron-donor (D) polymer and acceptor (A) fullerene is a promising technology for organic photovoltaics. Geminant charge recombination is regarded as one of the main loss mechanisms limiting device performances. This stems from the dynamics of the initial charge transfer state (CTS), which depend on the blend morphology, the molecular conformation, and the energetics of the D:A interface. Here we study the photophysics of a crystalline phase-separated blend of regioregular poly(3-hexylthiophene) (P3HT) with [6,6]-phenyl-C₆₁-butyric acid methyl ester (PCBM) with a coarsened morphology, by mapping the transient absorption signal with submicrometer space and subpicosecond time resolution. At the P3HT:PCBM interface, we detect a long-lived photoinduced dynamic that we assign to a peculiar coherent CTS forming in ~10 ps, not affected by geminant recombination and characterized by a different polarization with respect to the one in the usual polydisperse blend. Quantum chemical calculations on supramolecular P3HT:PCBM complexes confirm the presence of low-lying and highly polarized CTS, validating the experimental findings.



SECTION: Kinetics, Spectroscopy

A key challenge for improving bulk heterojunction (BHJ) solar cells performances, based on polymer:fullerene blends, is to develop a comprehensive understanding of the fundamental relationship between the morphology of the phase-separated blend and the photophysics of the excited states involved in the charge transfer process.^{1–5} In particular, extensive spectroscopic investigations have been carried out recently on the photophysics of the charge transfer state (CTS) at the molecular interface between polymers and fullerene derivatives.^{6–10} CTS consists of partially separated, Coulombically bound ($E_b = 0.1\text{--}0.5 \text{ eV} \gg k_B T^{11}$), charge pairs, where the hole is primarily localized on the donor (D) highest occupied molecular orbital (HOMO) and the electron on the acceptor (A) lowest unoccupied molecular orbital (LUMO).¹¹ Their wave function overlap results in the formation of hybrid ground and excited states, lying within the optical gap of the two materials. To describe such an intermediate state, different nomenclatures are often used such as bound polaron pair, bound electron hole pair, geminant pair, and CTS. In the following we are assuming that there is only one intermediate species, which we call the CTS. The branching between full ionization and geminant recombination of CTS is the main factor in determining the photovoltaic performances.^{12,13} In particular, it has been demonstrated that geminant recombination is the main loss channel limiting charge photogeneration efficiency

at short circuit condition, while the primary determinant of both the open-circuit voltage and fill factor of poly(3-hexylthiophene) (P3HT):[6,6]-phenyl-C₆₁-butyric acid methyl ester (PCBM) devices is bimolecular recombination.⁴ Owing to the confinement of CTSs at the boundaries between D/A phases, the nanoscale morphology dramatically affects their properties.^{13–17} Recent experimental investigations suggest that increasing phase segregation can reduce geminant recombination and improve the overall yield of charge photogeneration. In particular, the latest results demonstrated an improved separation of bound electron–hole pairs at D–A interfaces in P3HT:PCBM blends due to the formation of PCBM crystals.^{11,18–20} It was speculated that the high local mobility of hot electrons in these clusters (up to $0.2 \text{ cm}^2 \text{ V}^{-1} \text{ s}^{-1}$ in PCBM^{20,21}) might favor the formation of more spatially separated pairs after thermalization,^{5,22} but no clear evidence for the nature of the interface state could be reported. An interesting way to improve the BHJ efficiency is to manipulate the crystalline content in the blend.^{23–25} Here we artificially coarsened the blend structure to spatially resolved the photophysics of single P3HT:PCBM crystalline phases.

Received: March 22, 2011

Accepted: April 18, 2011



ACS Publications

© XXXX American Chemical Society

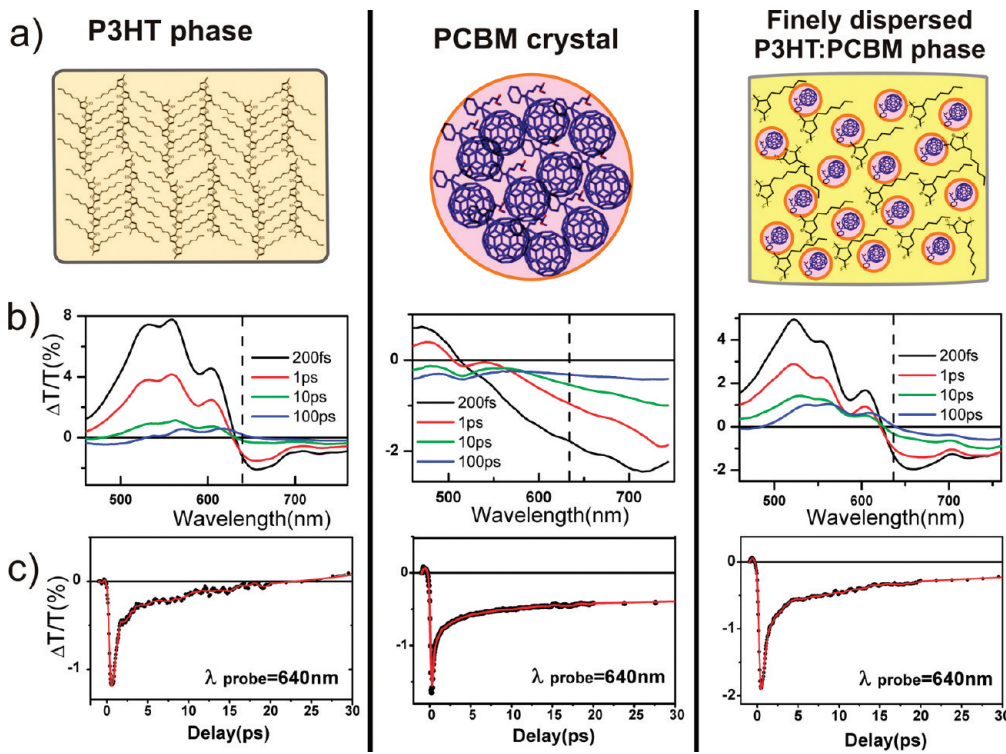


Figure 1. From left to right: (a) Scheme of crystalline P3HT phase, PCBM clusters, and finely dispersed annealed P3HT:PCBM (1:1) blend. (b) Related pump–probe spectra as measured on $\sim 150 \mu\text{m}$ spot and (c) temporal decay at $\lambda = 640 \text{ nm}$ probe wavelength (red curve superimposed on black dots).

We demonstrate that crystalline phases not only play a role in controlling the transport properties, but also affect the kinetics of charge separation/recombination after thermalization. We identify a peculiar long-lived CTS not affected by geminate recombination located at the border region between P3HT:PCBM microscopic phases: it displays a highly polarized component, and it is described by a quantum superposition of D and A states.

Thin films of P3HT:PCBM (weight ratio 1:1) were casted from a dichlorobenzene solution and thermally overannealed (see Section S2 in the Supporting Information for details). We tailored the degree of crystallization and phase separation by altering the film casting conditions and annealing process in order to obtain higher mesoscopic order and crystallinity within each phase.^{26,27} To better understand and compare the physical-chemical properties taking place upon blending, we investigate the photophysics of (*i*) P3HT-rich crystalline phase, (*ii*) PCBM-rich clusters, and (*iii*) P3HT:PCBM crystalline blends (as described above), by combining transient absorption spectroscopy with confocal microscopy, delivering simultaneously high temporal and spatial resolution. Briefly, our femtoscope is based on a homemade confocal microscope combined with an ultrafast pump–probe system, driven by $10 \mu\text{J}$, 150 fs pulses at 1 kHz repetition rate and 800 nm wavelength.²⁸ The pump beam (at $\lambda = 400 \text{ nm}$) and the probe one (white-light continuum spanning the 450–750 nm range) are temporally synchronized and sent into the confocal microscope, using a high numerical aperture air objective both for focusing and collection. The transmitted probe is then focused on the core of an optical fiber, used as the confocal pinhole. By raster scanning the sample position (x,y) and by varying the pump–probe delay (τ), we simultaneously acquire three-dimensional linear transmission $T(x,y,\lambda)$ and four-dimensional

differential transmission $\Delta T/T(x,y,\lambda,\tau)$ images with $\sim 150 \text{ fs}$ temporal and $\sim 300 \text{ nm}$ spatial resolution.

In Figure 1 standard pump–probe measurements (see Figure 1b) on both neat phases and finely dispersed blend (as schematically depicted in Figure 1a), are reported (see also paragraph S4 of the Supporting Information for details). Figure 1c represents the dynamics at $\lambda = 640 \text{ nm}$ probe wavelength for each case, useful as references for interpretation of the confocal signal. At $\lambda = 640 \text{ nm}$, the crystalline P3HT phase shows a photoinduced absorption (PA) signal, due to instantaneously photogenerated charge pairs that quickly recombine, overlapped with stimulated emission (SE), coming out at longer time scale, as visible from the dynamics of Figure 1c. PCBM clusters instead exhibit a PA due to singlet–singlet absorption (see Figure 1b).^{10,31,32} Interesting, in the P3HT:PCBM blend, a new decay channel for the neutral states becomes available, due to charge separation at the interface. The pump–probe spectrum of the finely dispersed blend (see Figure 1b) shows a longer lived PA band at [630–670 nm], assigned to the PA of Coulombically bounded CTS (note that free charge absorption occurs at longer wavelength side).^{10,31,32} The dynamic reveals a fast decay completed in 100 ps, mostly due to geminate recombination of CTS in the finely dispersed blend (see also Figure S3 in the Supporting Information for details).

The optical image (see Figure 2a) shows the coarsened P3HT:PCBM blend morphology made of single PCBM-rich crystals (whitish in Figure 2a) coexisting with submicrometer elongated P3HT-rich domains (darker in the optical image). Figure 2b shows the simultaneously collected $\Delta T/T$ map (pump–probe delay $\tau = 200 \text{ fs}$ and probe wavelength $\lambda = 640 \text{ nm}$); the image reveals regions of positive signal (red) embedded in a mainly negative one (blue). The positive region shows a long-lived

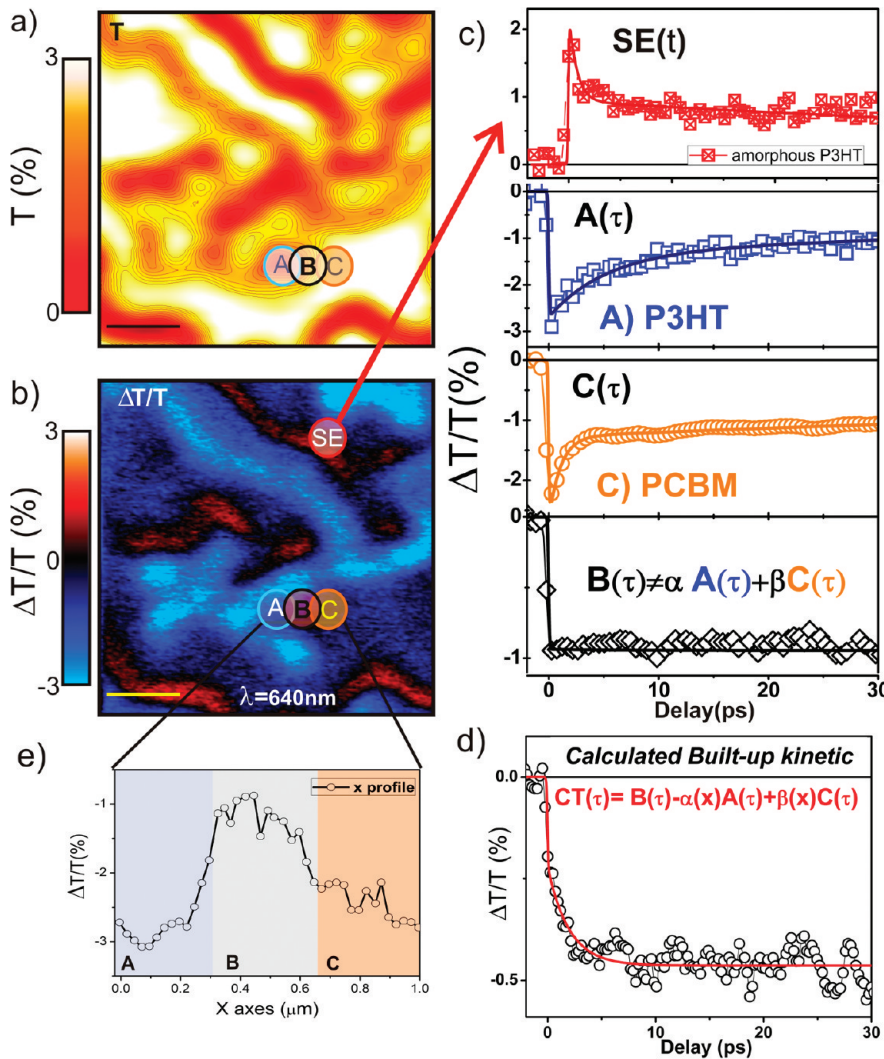


Figure 2. Linear transmission image (a) and $\Delta T/T(x,y)$ image (b) at $\lambda = 640$ nm and $\tau = 200$ fs pump–probe delay of a $5 \times 5 \mu\text{m}^2$ region; scale bar: $1 \mu\text{m}$. Excitation intensity $\sim 300 \text{ nJ}/\text{cm}^2$. (c) $\Delta T/T(\tau)$ dynamics at $\lambda = 640$ nm collected from (1) P3HT amorphous region (point SE in panel b) in red crossed squares; $\tau_1 = 1$ ps and $\tau_2 = 150$ ps are extracted by fitting the decay with a biexponential curve; (2) P3HT-rich crystal (point A) in blue squares; $\tau_1 = 8$ ps and $\tau_2 > 500$ ps are extracted by fitting the decay with a biexponential curve; (3) PCBMB-rich cluster (point C) in orange dots; $\tau_1 = 1.2$ ps and $\tau_2 > 250$ ps are extracted by fitting the decay with a biexponential curve; and (4) border region between crystallites (point B) black empty triangles; $\tau_1 = 12$ ps and $\tau_2 > 1$ ns are extracted by fitting the decay with a biexponential curve. (d) Extracted build-up CTS dynamic as $CT(\tau) = B(\tau) - \alpha \cdot A(\tau) + \beta \cdot C(\tau)$ at the interface. (e) Intensity trace profile of $\Delta T/T(x,y)$ signal across the interfacial region (named “B”) between a crystalline P3HT-rich phase (“A”) and a PCBMB-rich cluster (C). Note that the circular region would represent our confocal spot.

dynamic that we assign to SE signal coming from amorphous P3HT phase (as reported in panel 1 of Figure 2c).^{10,29–31} In this phase the singlet excitons do not dissociate, thus preventing the charge generation. In order to study the photophysics at the border region between different phases (P3HT:PCBM interfaces), we probe the spatially dependent signal (at $\lambda = 640$ nm probe wavelength) from a P3HT-rich crystal (named A in Figure 2a,b) to a PCBM-rich aggregate region (named C in Figure 2a,b). The intensity line trace is shown in Figure 2e. The collected dynamics in region A and C ($A(\tau)$ and $C(\tau)$, see panels 2 and 3 of Figure 2c, respectively) show a decay similar to the one collected from standard pump–probe measurements (see Figure 1c and the Supporting Information for details). Surprisingly, measuring the temporal decay at the border-region between the P3HT and PCBM rich-crystalline phases (named B in Figure 2a,b) we observe a steady PA signal, named $B(\tau)$ in the

following, which does not display any temporal evolution in the 300-ps observation window (see panel II in Figure 3).

This is striking evidence for the value added by the high spatial resolution of our femtoscope apparatus: such dynamics would have been washed out by any standard pump–probe measurement performed on a macroscopic sample area. The $\Delta T/T(\tau)$ signal collected from border regions (B) cannot be attributed by a linear superposition of simple spatial average of the two side border crystalline phases (in panels 2 and 3 of Figure 2c), because $B(\tau) \neq \alpha(x) \cdot A(\tau) + \beta(x) \cdot C(\tau)$, for any choice of the coefficients α, β , which depend on the actual lateral position between A and C. The difference between the two members of the inequality represents a new term, named $CT(\tau) = B(\tau) - \alpha(x) \cdot A(\tau) + \beta(x) \cdot C(\tau)$, as shown from the calculated values (black dots line) and fitted red curve in Figure 2d. We find the same result in many other border regions of our sample, and we

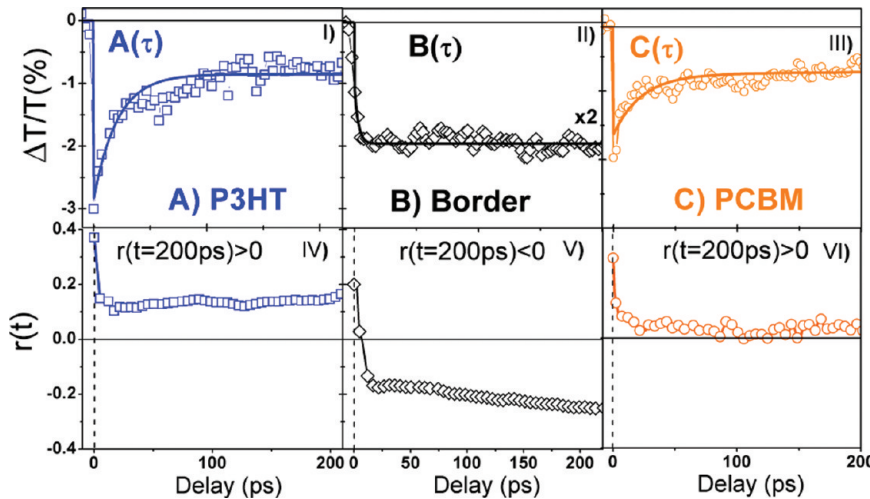


Figure 3. Long time-scale pump–probe dynamic and depolarization decay $r(\tau)$ at $\lambda = 640$ nm probe wavelength for the three different spots on the sample, previously identified at the P3HT-rich region (A) in panels I and IV, respectively; at the intercrystal border region (B) in panels II and V, respectively; and at the PCBM-rich cluster (C) in panels III and VI, respectively.

assign it to the formation of a peculiar long-lived CTS at the intercrystal region between the pure P3HT:PCBM phases. By fitting the decay with a biexponential, we extract a first-time constant of 12 ps and a second long-lived component >1 ns. The CTSs generated at the crystalline interface are long-lived, more than our accessible observation window, so that charge separation is expected to occur on the nanosecond time scale in kinetic competition with CT geminate recombination.⁵

In order to characterize the local electronic and molecular structure of CTS, to fully understand its physicochemical properties, we performed a combined experimental and theoretical study. By measuring polarization-dependent signal and the depolarization decay, we extract the transition dipole moment orientation of the involved excited CT states and their evolution. The sample depolarization ratio is given by eq 1:

$$r(\tau) = \frac{\frac{\Delta T}{T}(\tau)_{\text{par}} - \frac{\Delta T}{T}(\tau)_{\text{perp}}}{\frac{\Delta T}{T}(\tau)_{\text{par}} + 2\frac{\Delta T}{T}(\tau)_{\text{perp}}} \quad (1)$$

where $\Delta T/T(\tau)_{\text{par}}$ and $\Delta T/T(\tau)_{\text{perp}}$ represent the polarization of the pump and the probe beams, in a mutual parallel or cross configuration.⁹ Figure 3 displays the depolarization decay, reporting the values of r collected at $\lambda = 640$ nm probe wavelength and $\tau = 200$ ps delay. Remarkably, we find a spatial distribution of r , as illustrated in Figure S4 in the Supporting Information by mapping the anisotropy value, with regions displaying different absolute values and signs. The regions that we have previously marked as P3HT and PCBM rich-crystalline phase, named as A and C in Figure 3a, exhibit a positive r value (in the 0–0.2 range), which remains reasonably constant up to 200 ps (see panels IV and VI in Figure 3, respectively). The corresponding dynamics at cross-polarization are shown in panel I and III of Figure 3.

On the contrary, the depolarization decay measured at the border P3HT:PCBM region shows an initial positive polarization memory that quickly decays and changes sign, turning into a negative signal up to $r = -0.2$ (see panel V in Figure 3b). This peculiar depolarization dynamic is associated with regions localized at the interface between different phases, where a long-lived PA is detected (see panel II in Figure 3b). We conjecture that this

signal stems from the CTS. A negative value of $r(\tau)$ suggests a large tilt angle θ between the transition dipole moment of the probed transition with respect to the one induced by the pump, which can be evaluated according to the following equation:³³

$$r = \frac{2}{5} \left(\frac{3 \cos^2 \vartheta - 1}{2} \right) \quad (2)$$

We obtained $\theta = 90^\circ$. Such a large tilting occurs when strong interaction between D and A induces a mixing of the molecular wave functions, thus generating a new coherent state. At variance, weakly bound charge pairs would preserve the isolated properties. In this case, a polaron on a P3HT chain would show a transition moment along the chain. Our results instead indicate that the character of the long-lived CTS formed in between P3HT:PCBM crystal phases is different from that more commonly investigated in finely dispersed blends.

From our experimental results we measured a peculiar PA dynamic, showing that the generation of CTS at the border region between crystalline phases occurs on a few picoseconds time scale. This delay is consistent with the time needed for the singlets to diffuse before their dissociation at the interface. Considering a diffusion coefficient $D = 10^{-3}\text{--}10^{-4}$ cm²/s and the measured CTS formation time of $\tau = 10$ ps, we can extract the mean free path before dissociation $\lambda = 4D\tau^{1/2} \approx 2\text{--}10$ nm, representing the size of the effective D/A interface.³² This shows that the femtoscope, thanks to a combination of both high space and time resolution, is able to single out dynamics originating from a 20 nm area, much smaller than the diffraction-limited spot. The CTSs generated at the crystalline interfaces are long-lived, on a hundreds of picoseconds time scale, and exhibit a transition dipole moment strongly polarized perpendicularly respect to the P3HT chain.

To support our experimental evidence and validate the above conclusions, we performed a theoretical investigation aimed at modeling the P3HT:PCBM heterojunction.

Understanding the nature of CTS at the interface requires an accurate quantum chemical description of structural and electronic properties, as excellently reported in recent works by Brédas³⁴ and Troisi.³⁵ Herein the modeling has been carried

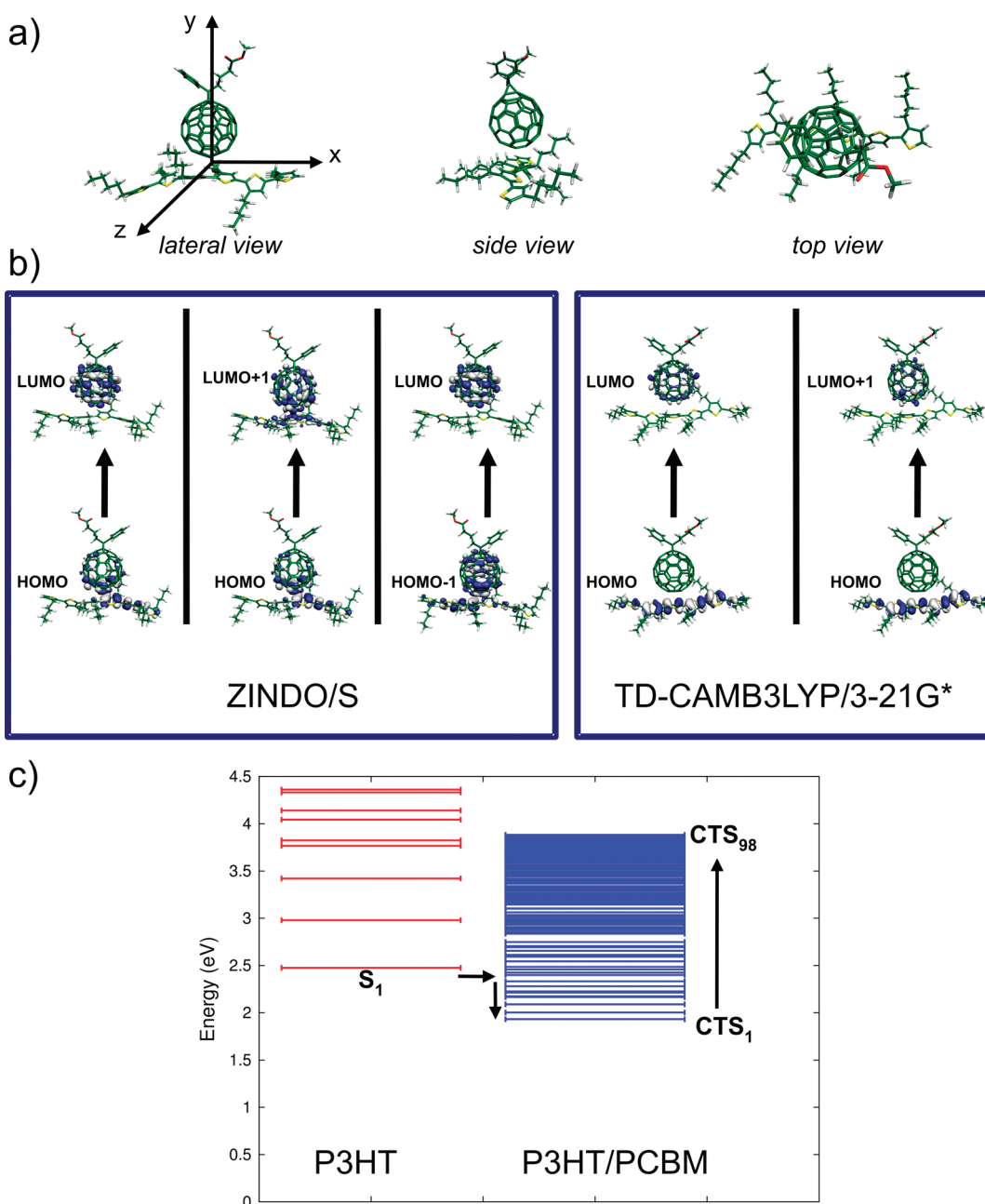


Figure 4. PCBM and P3HT interface. (a) Supramolecule (P3HT:PCBM) as obtained by separate optimization of PCBM and P3HT molecules; the optimized structures have been superimposed, at an intermolecular distance of $\sim 3.4\text{--}3.5\text{ \AA}$.^{36–40} Cartesian axes and projection planes are reported for clarity. (b) Left panel: isosurface molecular orbitals calculated at the singlet configuration interaction level (ZINDO/S), contributing to the electronic transition from the ground state to the low-lying excited state $|\text{CTS}_1\rangle$ of the P3HT:PCBM dimer. Right panel: TD-CAMB3LYP/3-21G* level of theory. (c) ZINDO/S excited states for isolated P3HT (red) and for P3HT:PCBM complex (blue) with a sketch of the possible photophysical mechanism herein studied.

out in order to qualitatively interpret the experimental results. The P3HT:PCBM interface has been modeled by considering supramolecule complexes formed by a PCBM face versus a P3HT oligomer^{36–40} (see Section S6 in the Supporting Information for more details), as reported in Figure 4a. Both ZINDO/S and TD-CAMB3LYP/3-21G* (and also 6-31G**) calculations (see Supporting Information for details) show that the lowest excited state of the P3HT:PCBM complex has an excitation energy (ZINDO/S: 1.93 eV, $f = 0.05$ a.u., TD-CAMB3LYP: 2.6 eV, $f = 0.001$) that is lower than those of the P3HT oligomer

(ZINDO/S: 2.47 eV, TD-CAMB3LYP: 3.3 eV) or the PCBM (ZINDO/S: 2.18 eV, TD-CAMB3LYP: 2.9 eV) molecule, as considered isolated (see section S6 in the Supporting Information for details). The calculated red shift of the dimer excited state energy and the small oscillator strength could be evidence of the formation of an “exciplex” state at the BHJ.³⁹ The identified low-lying excited state (e.g., $|\text{CTS}_1\rangle$) for the P3HT:PCBM complex, can be described as³⁹ $|\text{CTS}_1\rangle = c_{\text{CT}} |\text{A} \rightarrow \text{B}\rangle + c_{\text{EX}} |\text{A/B} \rightarrow \text{A/B}\rangle$, where $|\text{CTS}_1\rangle$ is the wave function of the lowest excited state, c_{CT} and c_{EX} are the coefficients weighting the charge

transfer and the local excitations character of $|CTS_1\rangle$ (A = P3HT and B = PCBM). In Figure 4b we report the dimer molecular orbitals describing the $|CTS_1\rangle$ state (both ZINDO/S and TD-CAMB3LYP results). The prevalent character of this excited state electronic configuration is the charge transfer from P3HT to PCBM (all the singlet configurations describing $|CTS_1\rangle$ are characterized by a LUMO mainly localized on the PCBM molecule); in ZINDO/S some contribution is also derived from the so-called bridging configuration,³⁷ where the P3HT/PCBM wave functions overlap across the interface, thus favoring the adiabatic electron transfer from P3HT to PCBM.^{5,37} Expanding $|CTS_1\rangle$ in a molecular orbital basis set,³⁹ the weight of the charge transfer character (c_{CT}) is around 0.75 for both ZINDO/S and TD-CAMB3LYP. The calculated transition dipole moment of $|CTS_1\rangle$ is polarized in the xz and xy planes (Figure 4a) showing an angle of 55° (ZINDO/S) or 65° (TD-CAMB3LYP), with respect to the P3HT chain. According to experimental results, a long-lived PA feature appears in the P3HT:PCBM BHJ around 630–670 nm (Figure 4c) as a fingerprint of the formation of CTS. We assign this PA band to electronic transitions of the P3HT:PCBM supramolecular complex from $|CTS_1\rangle$ to high-energy $|CTS_n\rangle$ states. In Figure 4c we report the calculated excited states for both the isolated P3HT oligomer and those for the P3HT:PCBM complex (more than 100 excited states evaluated at the ZINDO/S). In agreement with experimental data, theoretical simulations do confirm the CTS formation at the BHJ interface. Excitons formed in P3HT-rich crystalline phase (excited state S_1), migrate at the P3HT:PCBM interface and decay to the intermolecular $|CTS_1\rangle$ state. The $\lambda = 640$ nm probe can promote electronic transitions from $|CTS_1\rangle$ to $|CTS_n\rangle$ excited states. From ZINDO/S calculations, $|CTS_n\rangle$ states, located at ~ 1.94 eV (640 nm) above $|CTS_1\rangle$, show a strong charge transfer character. In particular, $|CTS_{98}\rangle$ (3.86 eV) is predicted to be polarized mainly perpendicular with respect to the P3HT chain direction, showing an angle of 70°. The calculated angle strongly supports the experimental evidence of an off-chain component resulting in a negative anisotropy value for the interfacial CTS (Figure 4b).

In conclusion, experiments and calculations on P3HT:PCBM blends bring evidence of a new CTS, localized at the interface between crystalline domains. Our results suggest that the initial CTS that forms at the crystallites border is a molecular dimer with intermixed character due to strong quantum superposition, i.e., a new coherent excited state with proper energy, polarization, and dynamics. The idea that higher mobility would favor the initial (after thermalization) large separation between charge pairs in the CTS seems incorrect. The absorption spectrum of those well-separated pairs would indeed appear as isolated polarons, contrary to our finding. We conclude that the role of the crystalline phase does not appear in the thermalization, but in two other processes: the initial diffusion of photoexcited states to the interface and perhaps the CT ionization. Both could benefit from better energy and charge migration, due to the crystalline order. This would lead to higher yield of CTS and lower geminate recombination. Note, however, that the real novelty here is the investigation of the physicochemical nature of the intercrystallite CTS and its long lifetime, which stems from the electronic properties of the dimer complex.

■ ASSOCIATED CONTENT

5 Supporting Information. Experimental setup, sample's details, additional pump–probe spectra and confocal map, and

details on theoretical calculations. This material is available free of charge via the Internet at <http://pubs.acs.org>.

■ AUTHOR INFORMATION

Corresponding Author

*E-mail: guglielmo.lanzani@iit.it.

■ ACKNOWLEDGMENT

D.P. would like to acknowledge financial support by the HFSP program Grant Number RGP0005 and the “5 per mille junior” research grant by Politecnico di Milano. J.C.-G. thanks the Spanish Ministry of Science and Innovation for funding through the Programa Ramon y Cajal. The work is partially supported by PRIN Project 2008 JKBBK4 “Tracking ultrafast photoinduced intra- and inter-molecular processes in natural and artificial photosensors”. D.F. thanks CILEA consortium for supercomputing facilities.

■ REFERENCES

- (1) Liang, Y.; Xu, Z.; Xia, J.; Tsai, S. T.; Wu, Y.; Li, G.; Ray, C.; Yu, L. For the Bright Future - Bulk Heterojunction Polymer Solar Cells with Power Conversion Efficiency of 7.4%. *Adv. Mater.* **2010**, *22*, E135–E138.
- (2) Scharber, M. C.; Koppe, M.; Gao, J.; Cordella, F.; Loi, M. A.; Denk, P.; Morana, M.; Egelhaaf, H. J.; Forberich, K.; Dennler, G.; Gaudiana, R.; Waller, D.; Zhu, Z.; Shi, X.; Brabec, C. J. Influence of the Bridging Atom on the Performance of a Low-Bandgap Bulk Heterojunction Solar Cell. *Adv. Mater.* **2010**, *22*, 367–370.
- (3) Benson-Smith, J. J.; Goris, L.; Vandewal, K.; Haenen, K.; Manca, J. V.; Vanderzande, D.; Bradley, D. D. C.; Nelson, J. Formation of a Ground-State Charge-Transfer Complex in Polyfluorene/[6,6]-Phenyl-C61 Butyric Acid Methyl Ester (PCBM) Blend Films and Its Role in the Function of Polymer/PCBM Solar Cells. *Adv. Funct. Mater.* **2007**, *17*, 451–457.
- (4) Shuttle, C. G.; Hamilton, R.; O'Regan, B. C.; Nelson, J.; Durrant, J. R. Charge-Density-Based Analysis of the Current–Voltage Response of Polythiophene/Fullerene Photovoltaic Devices. *Proc. Natl. Acad. Sci. U.S.A.* **2010**, *107*, 16448–16452.
- (5) Clarke, T. M.; Durrant, J. R. Charge Photogeneration in Organic Solar Cells. *Chem. Rev.* **2010**, *110*, 6736–6767.
- (6) Keivanidis, P. E.; Clarke, T. M.; Lilliu, S.; Agostinelli, T.; Macdonald, J. E.; Durrant, J. R.; Bradley, D. D. C.; Nelson, J. Dependence of Charge Separation Efficiency on Film Microstructure in Poly(3-hexylthiophene-2,5-diyl):[6,6]-Phenyl-C61 Butyric Acid Methyl Ester Blend Films. *J. Phys. Chem. Lett.* **2010**, *1*, 734–738.
- (7) Wang, X.; Zhang, D.; Braun, K.; Egelhaaf, H. J.; Brabec, C.; Meixner, A. High-Resolution Spectroscopic Mapping of the Chemical Contrast from Nanometer Domains in P3HT:PCBM Organic Blend Films for Solar-Cell Applications. *Adv. Funct. Mater.* **2010**, *20*, 492–499.
- (8) Hwang, I. W.; Moses, D.; Heeger, A. J. Photoinduced Carrier Generation in P3HT/PCBM Bulk Heterojunction Materials. *J. Phys. Chem. C* **2008**, *112* (11), 4350–4354.
- (9) Muller, J. G.; Lupton, J. M.; Feldmann, J.; Lemmer, U.; Scharber, M. C.; Sariciftci, N. S.; Brabec, C. J.; Scherf, U. Ultrafast Dynamics of Charge Carrier Photogeneration and Geminate Recombination in Conjugated Polymer:Fullerene Solar Cells. *Phys. Rev. B* **2005**, *72*, 195208-1–195208-10.
- (10) Ohkita, H.; Cook, S.; Astuti, Y.; Duffy, W.; Tierney, S.; Zhang, W.; Heeney, M.; McCulloch, I.; Nelson, J.; Bradley, D. D. C.; Durrant, J. R. Charge Carrier Formation in Polythiophene/Fullerene Blend Films Studied by Transient Absorption Spectroscopy. *J. Am. Chem. Soc.* **2008**, *130*, 3030–3042.
- (11) Veldman, D.; Meskers, C. J.; Janssen, R. A. J. The Energy of Charge-Transfer States in Electron Donor–Acceptor Blends: Insight

- into the Energy Losses in Organic Solar Cells. *Adv. Funct. Mater.* **2009**, *19*, 1939–1948.
- (12) Howard, I. A.; Mauer, R.; Meister, M.; Laquai, F. Effect of Morphology on Ultrafast Free Carrier Generation in Polythiophene: Fullerene Organic Solar Cells. *J. Am. Chem. Soc.* **2010**, *132*, 14866–14876.
 - (13) Veldman, D.; Ipek, O.; Meskers, S. C. J.; Sweelissen, J.; Koetse, M. M.; Veenstra, S. C.; Kroon, J. M.; van Bavel, S. S.; Loos, J.; Janssen, R. A. J. Compositional and Electric Field Dependence of the Dissociation of Charge Transfer Excitons in Alternating Polyfluorene Copolymer/Fullerene Blends. *J. Am. Chem. Soc.* **2008**, *130*, 7721–7735.
 - (14) McNeill, C. R.; Westenhoff, S.; Groves, C.; Friend, R. H.; Greenham, N. C. Influence of Nanoscale Phase Separation on the Charge Generation Dynamics and Photovoltaic Performance of Conjugated Polymer Blends: Balancing Charge Generation and Separation. *J. Phys. Chem. C* **2007**, *111* (51), 19153–19160.
 - (15) Clarke, T. M.; Ballantyne, A. M.; Nelson, J.; Bradley, D. D. C.; Durrant, J. R. Free Energy Control of Charge Photogeneration in Polythiophene/Fullerene Solar Cells: The Influence of Thermal Annealing on P3HT:PCBM Blends. *Adv. Funct. Mater.* **2008**, *18*, 4029–4035.
 - (16) Hallermann, M.; Kriegel, I.; Da Como, E.; Berger, J. M.; Von Hauff, E.; Feldmann, J. Charge Transfer Excitons in Polymer/Fullerene Blends: The Role of Morphology and Polymer Chain Conformation. *Adv. Funct. Mater.* **2009**, *19*, 3662–3668.
 - (17) Ballantyne, A. M.; Ferenczi, T. A. M.; Campoy-Quiles, M.; Clarke, T. M.; Maurano, A.; Wong, K. H.; Zhang, W. M.; Stingelin-Stutzmann, N.; Kim, J. S.; Bradley, D. D. C.; Durrant, J. R.; McCulloch, I.; Heeney, M.; Nelson, J.; Tierney, S.; Duffy, W.; Mueller, C.; Smith, P. U. Understanding the Influence of Morphology on Poly(3-hexylselenothiophene):PCBM Solar Cells. *Macromolecules* **2010**, *43*, 1169–1174.
 - (18) Yang, X.; Van Duren, J. K. L.; Janssen, R. A. J.; Michels, M. A. J.; Loos, J. Morphology and Thermal Stability of the Active Layer in Poly(p-phenylenevinylene)/Methanofullerene Plastic Photovoltaic Devices. *Macromolecules* **2004**, *37*, 2151–2158.
 - (19) Lee, J.; Ma, W. L.; Brabec, C. J.; Yuen, J.; Moon, J. S.; Kim, J. Y.; Lee, K.; Bazan, G. C.; Heeger, A. J. Processing Additives for Improved Efficiency from Bulk Heterojunction Solar Cells. *J. Am. Chem. Soc.* **2008**, *130*, 3619–3623.
 - (20) Kim, Y.; Choulis, S. A.; Nelson, J.; Bradley, D. D. C.; Cook, S.; Durrant, J. R. Device Annealing Effect in Organic Solar Cells with Blends of Regioregular Poly(3-hexylthiophene) and Soluble Fullerene. *Appl. Phys. Lett.* **2005**, *86*, 063502–063504.
 - (21) Cabanillas-Gonzalez, J.; Virgili, T.; Gambetta, A.; Lanzani, G.; Anthopoulos, T. D.; de Leeuw, D. M. Photoinduced Transient Stark Spectroscopy in Organic Semiconductors: A Method for Charge Mobility Determination in the Picosecond Regime. *Phys. Rev. Lett.* **2006**, *96*, 106601–106604.
 - (22) Grzegorczyk, W. J.; Savenije, T. J.; Heeney, M.; Tierney, S.; McCulloch, I.; van Bavel, S.; Siebbeles, L. D. A. Relationship between Film Morphology, Optical, and Conductive Properties of Poly(thienothiophene):[6,6]-Phenyl C-61-Butyric Acid Methyl Ester Bulk Heterojunctions. *J. Phys. Chem. C* **2008**, *112*, 15973–15979.
 - (23) Campbell, A. R.; Hodkiss, J. M.; Westenhoff, S.; Howard, I. A.; Marsh, R. A.; McNeill, C. R.; Friend, R.; Greenham, N. C. Low-Temperature Control of Nanoscale Morphology for High Performance Polymer Photovoltaics. *Nano Lett.* **2008**, *8*, 3942–3947.
 - (24) McNeill, C. R.; Abrusci, A.; Hwang, I.; Ruderer, M. A.; Muller-Buschbaum, P.; Greenham, N. C. Photophysics and Photocurrent Generation in Polythiophene/Polyfluorene Copolymer Blends. *Adv. Funct. Mater.* **2009**, *19*, 3103–3111.
 - (25) Dennler, G.; Scharber, M. C.; Brabec, C. J. Polymer–Fullerene Bulk-Heterojunction Solar Cells. *Adv. Mater.* **2009**, *21*, 1323–1338.
 - (26) Campoy-Quiles, M.; Ferenczi, T.; Agostinelli, T.; Etchegoin, P. G.; Kim, Y.; Anthopoulos, T. D.; Stavrinou, P. N.; Bradley, D. D. C.; Nelson, J. Morphology Evolution via Self-Organization and Lateral and Vertical Diffusion in Polymer:Fullerene Solar Cell Blends. *Nat. Mater.* **2008**, *7*, 158–164.
 - (27) Swinnen, A.; Haeldermans, I.; Vande Ven, M.; D'Haen, J.; Vanhooyland, G.; Aresu, S.; D'Olieslaeger, M.; Manca, J. Tuning the Dimensions of C₆₀-Based Needlelike Crystals in Blended Thin Films. *Adv. Funct. Mater.* **2006**, *16*, 760–765.
 - (28) Polli, D.; Grancini, G.; Clark, J.; Celebrano, M.; Virgili, T.; Cerullo, G.; Lanzani, G. Nanoscale Imaging of the Interface Dynamics in Polymer Blends by Femtosecond Pump–Probe Confocal Microscopy. *Adv. Mater.* **2010**, *22*, 3048–3051.
 - (29) Marsh, R. A.; Hodkiss, J. M.; Albert-Seifried, S.; Friend, R. Effect of Annealing on P3HT:PCBM Charge Transfer and Nanoscale Morphology Probed by Ultrafast Spectroscopy. *Nano Lett.* **2010**, *10*, 923–930.
 - (30) Guo, J.; Ohkita, H.; Benten, H.; Ito, S. Near-IR Femtosecond Transient Absorption Spectroscopy of Ultrafast Polaron and Triplet Exciton Formation in Polythiophene Films with Different Regioregularities. *J. Am. Chem. Soc.* **2009**, *131*, 16869–16880.
 - (31) Guo, J.; Ohkita, H.; Benten, H.; Ito, S. Charge Generation and Recombination Dynamics in Poly(3-hexylthiophene)/Fullerene Blend Films with Different Regioregularities and Morphologies. *J. Am. Chem. Soc.* **2010**, *132*, 6154–6164.
 - (32) Cabanillas-Gonzalez, J.; Gambetta, A.; Zavelani-Rossi, M.; Lanzani, G. Kinetics of Interfacial Charges in Hybrid GaAs/Oligothiophene Semiconducting Heterojunctions. *Appl. Phys. Lett.* **2007**, *91*, 122113–122115.
 - (33) Valeur, B. *Molecular Fluorescence: Principles and Applications*; Wiley-VCH: Weinheim, Germany, 2002.
 - (34) Yi, Y.; Coropceanu, V.; Brédas, J. L. A Comparative Theoretical Study of Exciton-Dissociation and Charge-Recombination Processes in Oligothiophene/Fullerene and Oligothiophene/Perylenediimide Complexes for Organic Solar Cells. *J. Mater. Chem.* **2011**, *21*, 1479–1486.
 - (35) Liu, T.; Troisi, A. Absolute Rate of Charge Separation and Recombination in a Molecular Model of the P3HT/PCBM Interface. *J. Phys. Chem. C* **2011**, *115*, 2406–2415.
 - (36) Marchiori, C. F. N.; Koehler, M. Dipole Assisted Dissociation at Conjugated Polymer/Fullerene Photovoltaic Interfaces: A Molecular Study Using Density Functional Theory Calculations. *Synth. Met.* **2010**, *160*, 643–650.
 - (37) Kanai, Y.; Grossman, J. C. Insights on Interfacial Charge Transfer Across P3HT/Fullerene Photovoltaic Heterojunction From Ab Initio Calculations. *Nano Lett.* **2007**, *7*, 1967–1972.
 - (38) Yi, Y.; Coropceanu, V.; Brédas, J. L. Exciton-Dissociation and Charge Recombination Processes in Pentacene/C₆₀ Solar Cells: Theoretical Insight into the Impact of the Interface Geometry. *J. Am. Chem. Soc.* **2009**, *131*, 15777–15783.
 - (39) Huang, Y.; Westenhoff, S.; Avilov, I.; Sreearunothai, P.; Hodkiss, J. M.; Deleener, C.; Friend, R. H.; Beljonne, D. Electronic Structures of Intercalated States Formed at Polymeric Semiconductor Heterojunctions. *Nat. Mater.* **2008**, *7*, 483–489.
 - (40) Brédas, J. L.; Norton, J. E.; Cornil, J.; Coropceanu, V. Molecular Understanding of Organic Solar Cells: The Challenges. *Acc. Chem. Res.* **2009**, *42*, 1691–1699.